Spectroscopic Study of the EutT Adenosyltransferase from *Listeria monocytogenes*: Evidence for the Formation of a Four-Coordinate Cob(II)alamin Intermediate.

Nuru G. Stracey[a], Flavia G. Costa[b], Jorge C. Escalante-Semerena[b], and Thomas C. Brunold[a*]

[a]Department of Chemistry University of Wisconsin-Madison, Madison WI 53706
[b]Department of Microbiology, University of Georgia, Athens, GA 30602
Running title: Spectroscopic Studies of the EutT Adenosyltransferase from *Salmonella enterica*

Funding Source: This work was supported in part by the National Science Foundation grant CHE-1710339 to T.C.B. and the National Institutes of Health grant R37-GM40313 to J.C.E.-S.

*Corresponding author

1101 University Ave

Madison, WI 53706

Phone: (608) 265-9056

Fax: (608) 262-6143

brunold@chem.wisc.edu

ABSTRACT

The EutT enzyme from *Listeria monocytogenes* (*Lm*EutT) is a member of the family of ATP:cobalt(I) corrinoid adenosyltransferase (ACAT) enzymes that catalyze the biosynthesis of adenosylcobalamin (AdoCbl) from exogenous Co(II)rrinoids and ATP. Apart from EutT-type ACATs, two evolutionary unrelated types of ACATs have been identified, termed PduO and CobA. Although the three types of ACATs are non-homologous, they all generate a four-coordinate cob(II)alamin (4C Co(II)Cbl) species to facilitate the formation of a supernucleophilic Co(I)Cbl intermediate capable of attacking the 5'-carbon of co-substrate ATP. Previous spectroscopic studies of the EutT ACAT from *Salmonella enterica* (*Se*EutT) revealed that this enzyme requires a divalent metal cofactor for the conversion of 5C Co(II)Cbl to a 4C species. Interestingly, *Lm*EutT does not require a divalent metal cofactor for catalytic activity, which exemplifies an interesting phylogenetic divergence amongst the EutT enzymes. To explore if this disparity in metal cofactor requirement amongst EutT enzymes correlates with differences in substrate specificity or the mechanism of Co(II)Cbl reduction, we employed various spectroscopic techniques to probe the interaction of Co(II)Cbl and cob(II)inamide ($Co(II)Cbi^+$) with *Lm*EutT in the absence and presence of co-substrate ATP. Our data indicate that *Lm*EutT displays a similar substrate specificity as *Se*EutT and can bind both Co(II)Cbl and $Co(II)Cbi^+$ when complexed with MgATP, though exclusively converts Co(II)Cbl to a 4C species. Notably, *Lm*EutT is the most effective ACAT studied to date in generating the catalytically relevant 4C Co(II)Cbl species, achieving a >98% 5C→4C conversion yield on addition of just over one molar equivalent of co-substrate MgATP.

INTRODUCTION

Ethanolamine and 1, 2-propanediol can be utilized by bacteria as a source of carbon, nitrogen, and energy for metabolic function.[1-4] Pathogenic bacteria such as *Listeri*a, *Escherichia*, *Clostridium*, and *Salmonella* obtain ethanolamine from phosphatidylethanolamine, a phospholipid found in cell membranes,[5, 6] where it is broken down by phosphodiesterases into ethanolamine and glycerol.[1, 7, 8] The primary step in ethanolamine catabolism is catalyzed by ethanolamine ammonia-lyase (EAL) enzymes that convert ethanolamine into ammonia and acetaldehyde.[9] These molecules can then serve as a source of reduced nitrogen and a precursor to metabolically active acetyl-CoA, respectively.[10] Ethanolamine degradation by EAL involves a radical-based 1-2 elimination reaction mediated by adenosylcobalamin (AdoCbl), a corrinoid cofactor (Figure 1).[11-13] AdoCbl is supplied to apo-EAL by an ATP:Co(I)rrinoid adenosyltransferase (ACAT) enzyme encoded by the *eutT* gene.[1]

ACATs catalyze the biosynthesis of AdoCbl from exogenous Co(II)rrinoids and ATP.[14] Apart from EutT-type ACATs, two evolutionary unrelated types of ACATs have been identified, referred to as PduO and CobA. PduO-type ACATs are reported to play a similar role as EutT does in bacterial growth, supplying AdoCbl to the diol dehydratase associated with 1,2-propanediol metabolism.[15-17] CobA-type ACATs serve a housekeeping role and are responsible for adenosylating corrinoid precursors in *de novo* cobalamin biosynthesis and maintaining adequate intracellular levels of AdoCbl.[18, 19] Unlike the PduO- and CobA-type ACATs, EutT from *Salmonella enterica* (*Se*EutT) requires a divalent metal ion [Fe(II) or Zn(II)] for activity that is postulated to reside in a tetrahedral coordination environment provided by four Cys residues, which are part of a conserved $HX_{11}CCX_2C(83)$ motif.[20-22] Although the three types of ACATs are non-homologous, they all generate a four-coordinate (4C) cob(II)alamin (Co(II)Cbl) species to

facilitate the formation of a supernucleophilic Co(I)Cbl intermediate. This species is sufficiently potent to attack the 5'-carbon of ATP, so as to generate the Co–C(ATP) bond of AdoCbl.[23-27] The formation of a unique 4C Co(II)Cbl species in the presence of co-substrate ATP was initially proposed on the basis of electron paramagnetic (EPR) and magnetic circular dichroism (MCD) spectroscopic studies,[26, 28-30] and has since been confirmed by X-ray crystallographic studies of PduO from *Lactobacillus reuteri* (*Lr*PduO) and CobA from *Salmonella enterica* (*Se*CobA, Figure 2).[16, 31] In both structures the DMB base is solvent exposed and the lower axial position is blocked off by hydrophobic residues in the active site. Thus, even though the reduction potentials of free Co(II)rrinoids are substantially lower than those of biologically available reductants such as dihydroflavins (FMN) [e.g., E°(NHE) for Co(II)Cbl = –610 mV vs –228 mV for FMN at pH 7.5],[20, 32, 33] the generation of 4C Co(II)rrinoid species in the ACAT active sites raises the Co(II)/Co(I)corrinoid reduction potential to within the physiologically accessible range.[28, 29, 34]

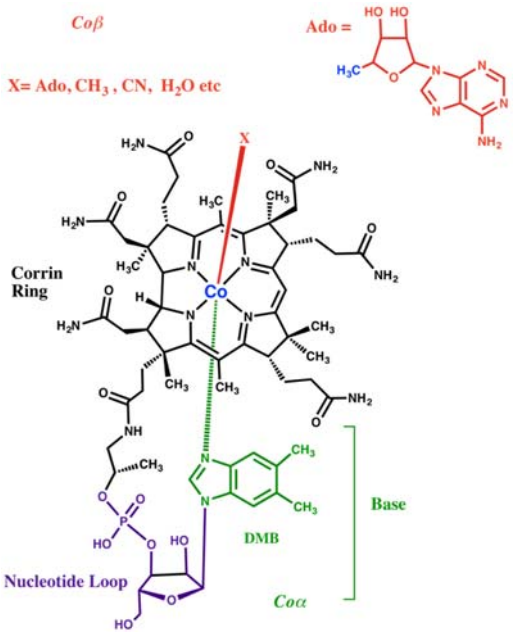

Figure 1. Chemical structure of cob(III)alamin species. In AdoCbl, the variable "upper" axial ligand, X, is Ado as indicated. In cob(III)inamide species the negatively charged nucleotide loop with the DMB base is absent, which causes a water molecule to bind in the "lower" axial

position. Upon Co(III)→Co(II) reduction of cob(III)alamin and cob(III)inamide species, the upper axial ligand is lost to generate the five-coordinate, neutral cob(II)alamin [Co(II)Cbl] and mono-cationic cob(II)inamide [Co(II)Cbi$^+$] species.

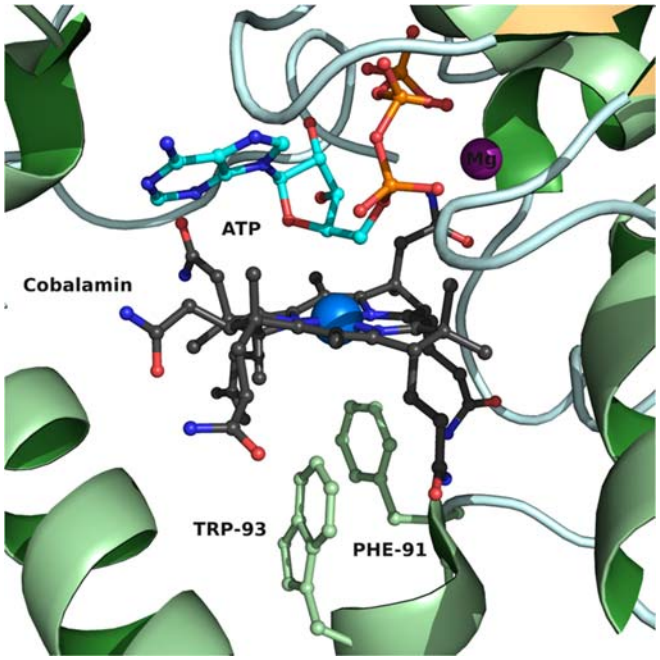

Figure 2. X-ray crystal structure of 4C Co(II)Cbl (black) in the active site of *Se*CobA, with Mg-ATP located above the corrin ring. Key hydrophobic residues are indicated (pale green) that block off the lower axial position. Note that the DMB base, aminopropanol linkage and nucleotide loop are not resolved in the crystal structure as they are likely solvent exposed.[31]

Although thus far no member of the EutT family has been characterized by X-ray crystallography, MCD and EPR studies of *Se*EutT revealed that this enzyme also generates a 4C Co(II) species to facilitate substrate reduction.[24, 27] These studies have also served to highlight key differences in the selectivity and mode of 4C Co(II)rrinoid formation between the different ACAT families. *Lr*PduO and *Se*CobA can convert both Co(II)Cbl and cob(II)inamide (Co(II)Cbi$^+$, which lacks the nucleotide loop with the terminal DMB base and therefore binds a water molecule in the "lower" axial position) to 4C species that are readily reduced to the Co(I) state. In contrast, *Se*EutT is only

able to convert Co(II)Cbl to a 4C species. This is surprising considering that the Co–OH_2 bond of Co(II)Cbi^+ is significantly weaker than the Co–DMB bond of Co(II)Cbl.[23-27] Spectroscopic studies of *Se*EutT revealed that the divalent metal ion is essential for the conversion of Co(II)Cbl to a 4C species, presumably by properly organizing a putative DMB binding pocket.[24] However, the EutT enzyme from *Listeria monocytogenes* (*Lm*EutT) lacks this divalent metal-binding motif, which exemplifies an interesting phylogenetic divergence amongst the EutT enzymes. As *Lm*EutT does not require a divalent metal cofactor for activity, we sought to expand our understanding of the catalytic mechanisms employed by ACATs through spectroscopic studies of this enzyme. Specifically, we have employed electronic absorption (Abs), MCD, and EPR spectroscopic techniques to probe the interaction of Co(II)Cbl and Co(II)Cbi^+ with *Lm*EutT in the absence and presence of co-substrate ATP.

MATERIALS AND METHODS

Cofactors and chemicals

Dicyanocobinamide [$(CN)_2$Cbi], hydroxocobalamin hydrochloride [HOCbl·HCl], sodium borohydride ($NaBH_4$), and potassium formate (HCOOK) were purchased from Sigma Aldrich and used without further purification. Diaquacobinamide $(H_2O)_2Cbi^{2+}$ was prepared from $(CN)_2$Cbi according to the following procedure. About 3-5 mg of $(CN)_2$Cbi were dissolved in 5 mL MilliQ water and sparged for 60 min with N_2. The red/purple solution was then transferred via cannula to a sealed vial containing ~27 mg $NaBH_4$ and left stirring overnight under a slow stream of N_2. The resulting brown/purple solution was re-oxidized in air over several hours. Once fully oxidized, the solution was loaded onto a C18 Sep Pak column, washed with (i) ultrapure water (30 mL), (ii) a 20% methanol solution until the orange-colored band moved towards the eluting end of the

column, and (iii) again with ultrapure water (10 mL), and finally eluted with 100% methanol. Purified $(H_2O)_2Cbi^{2+}$ was collected under vacuum. Co(II)Cbl and $Co(II)Cbi^{+}$ were generated anaerobically by reduction of aqueous solutions of HOCbl and $(H_2O)_2Cbi^{2+}$ with ~40-60 μL of a saturated solution of HCOOK. The progress of the reduction was monitored spectrophotometrically.

Protein preparation and purification

*Lm*EutT was prepared as described elsewhere.[35] In short, BL21-CodonPlus cells (Agilent) containing pEUT140 (pTEV18 with *Lm*EutT) were grown at 37 ºC in 4 L flasks with metal springs containing 2 L of Terrific Broth media.[36] At an OD_{600} = 0.5-0.6, *eutT* gene expression was induced with 1 mM β-D-1-thiogalactopyranoside and the culture was incubated at 15 ºC for 30 hours. The harvested cells were pelleted at 6,000 x *g* in a refrigerated Avanti J-20 XPI with a JLA 8.1 rotor and re-suspended at 4 ºC in buffer A [50 mM, 2-[4-(2-hydroxyethyl)piperazin-1-yl]ethanesulfonic acid (HEPES), 500 mM NaCl, 1 mM tris(2-carboxyethyl)phosphine (TCEP), and 20 mM imidazole, pH 7.5] with 1 mg/mL lysozyme and 0.1 mg/mL DNase. The suspension was subsequently passed through a cell press at 1.91 kPa and phenylmethysulfonyl fluoride (PMSF, 1 mM) was added immediately after lysis. This sample was centrifuged in an Avanti J-25I centrifuge equipped with a JA 25.50 rotor at 40,000 x *g* for 30 min at 4 ºC and filtered with a 0.45 μm filter. The collected lysate was loaded onto a 5 mL HisTrap Fast Flow (GE) column equilibrated with buffer A. Protein was eluted with an imidazole gradient (20-500). The His_6-tag was cleaved by incubating the solution with recombinant tobacco etch virus (rTEV) protease[37] for 3 hours at room temperature, and the resulting protein sample was dialyzed three times against 1 L of buffer A. Further purification was achieved by loading protein onto the same column re-equilibrated with buffer A and collecting the flow-through. The collected fractions were concentrated to a protein

concentration of 1.1 mM and dialyzed three times against storage buffer (20 mM phosphate buffer, 200 mM NaCl, pH 7.5) at 4 ºC. The purity of the protein was determined using an SDS-PAGE gel and by analyzing the data with a 1D gel analysis software.

Sample preparation

Under anoxic conditions in a glove box, purified protein samples (300-700 μM) in 20 mM phosphate buffer with 200 mM NaCl at pH 7.5 were mixed with 55-60% (v/v) glycerol and complexed with Co(II)Cbl or $Co(II)Cbi^+$ at a cofactor to protein ratio of 0.9:1 (for MCD) or 0.7:1 (for EPR). Varying equivalents of MgATP were added to the different MCD and EPR samples, as noted in the corresponding figure captions. The solutions were then injected into MCD sample cells or EPR tubes and frozen in liquid nitrogen (LN_2) either immediately (EPR samples) or after collecting room temperature Abs data (MCD samples).

Spectroscopy

X-band EPR spectra were collected on a Bruker ESP 300E spectrometer equipped with an Oxford ESR 900 continuous-flow liquid helium cryostat and an Oxford ITC4 temperature controller. All spectra were collected at 20 K using the following instrument settings: frequency = 9.38 GHz, microwave power = 2.0 mW, gain = 40-60 dB, modulation amplitude = 5 G, conversion time = 87 ms, time constant = 327.68 ms, range = 600-4598 G, resolution = 2048 points and modulation frequency = 100kHz. Simulated EPR spectra were fitted using the SIMPOW program written by Dr. Mark Nilges.[38]

Room temperature Abs spectra were obtained using a Varian Cary 5e spectrophotometer. The sample compartment was purged with $N_2(g)$ for 40 min prior to data collection. Frozen solution Abs and MCD spectra were collected with a JASCO J-715 spectropolarimeter in conjunction with an Oxford Instruments SM-4000 8 T superconducting magnetocryostat. Circular

dichroism and glass-strain contributions to the MCD spectra were removed by taking the difference between spectra obtained with the magnetic field oriented parallel and anti-parallel to the light of propagation axis. Sample conditions are listed in the caption of each figure.

RESULTS

Abs and MCD Data. To probe the interaction between the corrinoid substrate and the *Lm*EutT active site, we have conducted a series of Abs, MCD and EPR spectroscopic studies of Co(II)Cbl and Co(II)Cbi$^+$ in the absence and presence of *Lm*EutT both before and after the addition of co-substrate MgATP. The 4.5 K Abs spectrum of free, 5C base-on Co(II)Cbl in aqueous solution is dominated by intense features associated primarily with $\pi \rightarrow \pi^*$ transitions localized on the corrin ring (Figure 3A). The prominent feature at ~21 000 cm^{-1} (~476 nm), referred to as the α band, was previously assigned as the lowest energy corrin-based $\pi \rightarrow \pi^*$ transition, while the steady increase in Abs intensity between 17 000 and 19 000 cm^{-1} was attributed to metal-to-ligand charge transfer (MLCT) transitions involving the occupied Co(II) 3d- and empty corrin π^*-based molecular orbitals (MOs).[39, 40] In the corresponding MCD spectrum, at least two positively signed features are present this region. Additionally, several derivative-shaped MCD features are observed between 14 000 and 17 000 cm^{-1} that were assigned as electronic excitations from the doubly occupied Co $3d_{xz}$ and $3d_{yz}$ based-MOs to the singly occupied, "redox active" Co-$3d_{z^2}$-based MO based on time-dependent density functional theory (TD-DFT) calculations.[39, 41, 42]

When a small excess of *Lm*EutT was added to a sample of Co(II)Cbl, the low-temperature (LT) Abs and MCD spectra changed minimally (Figure 3B), indicating that Co(II)Cbl may not bind to the *Lm*EutT active site in the absence of co-substrate MgATP. In contrast, upon the addition of a slight excess (1.3 equiv.) of MgATP to a sample containing Co(II)Cbl and *Lm*EutT in a 0.9:1.0

molar ratio, an immediate color change (from orange-red to yellow) was observed that correlates with the blue-shift of the α band in the LT Abs spectrum by ~500 cm^{-1} (to 464 nm, Figure 3C). As the donor MO for the α band transition has a significant antibonding contribution from the Co $3d_{z^2}$ and N(DMB) $2p_z$ orbitals, a blue shift of the α band is symptomatic of a weakening of the axial Co-ligand bond.[24, 29, 42] The magnitude of this blue-shift is marginally smaller (by ~33 cm^{-1}) than the corresponding shift observed when Co(II)Cbl binds to the *Se*EutT/MgATP complex, but larger (by ~100 cm^{-1}) than those reported for Co(II)Cbl binding to *Lr*PduO/MgATP and *Se*CobA/MgATP.

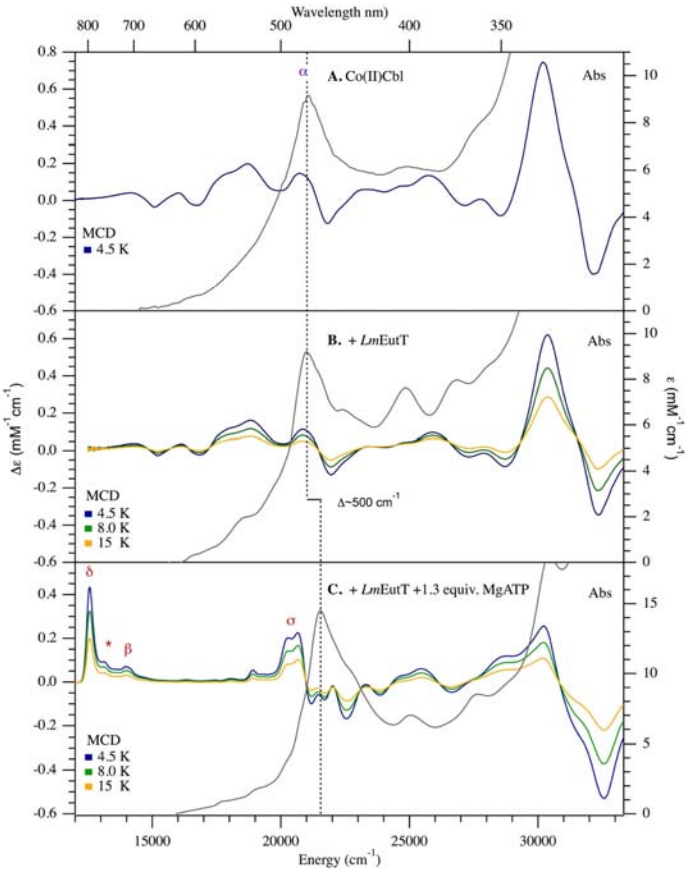

Figure 3. Abs spectra at 4.5 K (gray traces) and variable temperature MCD spectra at 7 T of (**A**) free Co(II)Cbl, **B**) Co(II)Cbl in the presence of *Lm*EutT and **C**) Co(II)Cbl in the presence of *Lm*EutT and 1.3 equiv MgATP. The dashed vertical line indicates the position of the α band.

The MCD spectrum of Co(II)Cbl bound to the *Lm*EutT/MgATP complex is characteristic of 4C Co(II)rrinoid species. On the basis of previous studies,[23, 24, 26, 27] the sharp features below 15 000 cm^{-1} can be attributed to the electronic origin (δ band at 12 560 cm^{-1}) and a vibrational sideband (β band at 14 014 cm^{-1}) associated with the $3d_{x2-y2} \rightarrow 3d_{z2}$ LF transition of 4C Co(II)Cbl.[23] The weak feature at 13 144 cm^{-1} (highlighted by *) likely corresponds to the first member of a vibrational progression involving a ~575 cm^{-1} corrin mode.[43] Conversely, the high energy (> 20 000 cm^{-1}) region is characterized by broad, both positively and negatively signed features that can be attributed to MLCT and $\pi \rightarrow \pi^*$ transitions.[25, 29] The lack of any residual features from 5C base-on Co(II)Cbl in these spectra reveals that nearly full (> 98%) conversion of the 5C base-on Co(II)Cbl to a 4C species occurred. Intriguingly, this near complete conversion at just over 1 equiv. of MgATP observed for *Lm*EutT is unprecedented, as neither *Se*EutT nor any of the other ACATs studied to date achieve such a high conversion yield even in the presence of excess MgATP.

Because the Abs spectra of corrinoids are dominated by features originating from corrin-based $\pi \rightarrow \pi^*$ transitions, it is unsurprising that the Abs spectrum of free $Co(II)Cbi^+$ is similar to that of Co(II)Cbl (Figure 4A). Yet, the MCD spectra of free $Co(II)Cbi^+$ and Co(II)Cbl are markedly different, which reflects differences in the Co 3d orbital splittings and highlights the power of this technique to probe geometric changes around the metal center of Co(II)rrinoid species. Upon incubation of $Co(II)Cbi^+$ with *Lm*EutT, no changes to the MCD spectrum are apparent, indicating that *Lm*EutT, like *Se*EutT,[24] is unable to bind $Co(II)Cbi^+$ in the absence of ATP (Figure 4B**)**. Even when a large excess (10 equiv.) of MgATP was added to a $Co(II)Cbi^+$ sample incubated with *Lm*EutT, the color remained unchanged and minimal changes to the Abs spectrum were observed (Figure 4C). However, close inspection of the corresponding MCD spectra reveals that the $Co(II)Cbi^+$ does in fact interact with the enzyme, as evidenced by the modest (~295 cm^{-1}) red-shift

of the lowest energy feature centered at 16 388 cm^{-1} (Figure 4C) that can be attributed to a slight elongation of the lower axial Co–OH_2 bond.[29] Overall, these data provide compelling evidence that *Lm*EutT, similar to *Se*EutT,[24] is unable to convert Co(II)Cb^+ to a 4C species.

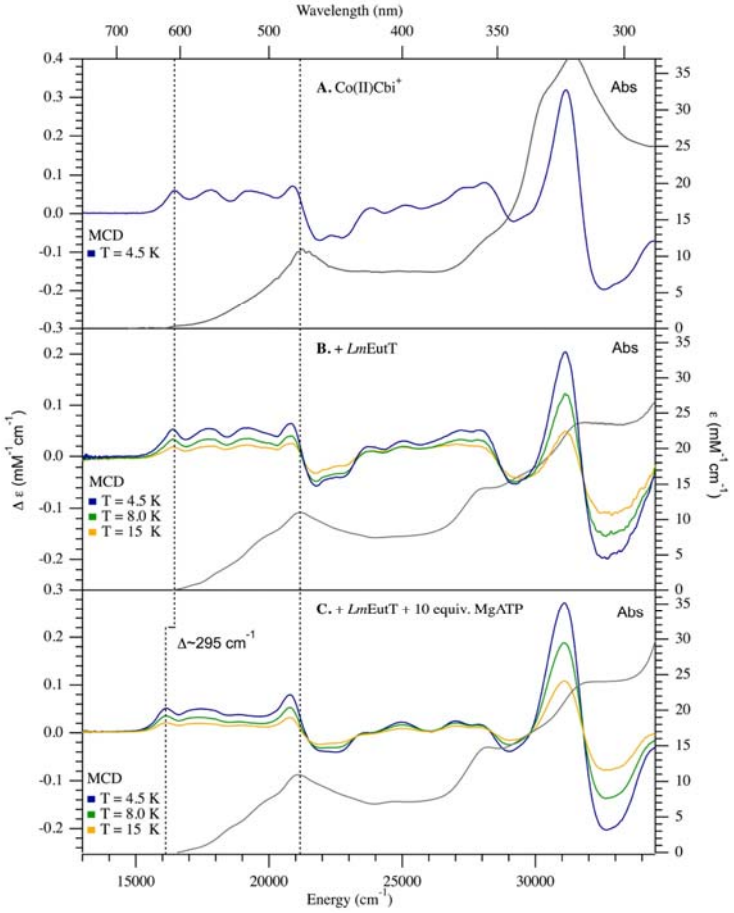

Figure 4. Abs spectra at 4.5 K (gray traces) and variable temperature MCD spectra at 7 T of **A**) free Co(II)Cbi^+, **B**) Co(II)Cbi^+ in the presence of *Lm*EutT **C**) Co(II)Cbi^+ in the presence of *Lm*EutT with 1.3 equiv. MgATP. The vertical lines indicate the position of the α band in the Abs spectra and the shift of the lowest energy feature in the MCD spectra.

EPR Data. To complement our electronic Abs and MCD data, we performed parallel studies using X-band EPR spectroscopy. As the unpaired electron of Co(II)Cbl and Co(II)Cbi^+ resides in the Co

$3d_{z^2}$–based MO, EPR spectroscopy is uniquely sensitive to changes in the axial ligation of the Co(II) ion.[25, 39, 44] Consistent with our MCD data, the EPR spectra of Co(II)Cbl in the absence and the presence of *Lm*EutT are essentially identical (Figure 5A and 5B), with small *g* spreads and a broad, derivative-shaped feature centered at 2973 G. Fine structure arising from both ^{59}Co hyperfine coupling [A(Co) = 30, 40 and 305 Hz] and axial ^{14}N superhyperfine coupling [$A_z(N^{14})$ = 40 MHz] are clearly visible between 3000 and 3700 G. Upon addition of 1.3 equiv. MgATP to Co(II)Cbl incubated with *Lm*EutT, large changes to the EPR spectrum are observed, with numerous weak features appearing in the range between 600 and 4600 G (Figure 5C and Table 1). On the basis of previous studies of other ACATs, these changes can be attributed to the loss of the axial DMB ligand from the Co(II) ion, which leads to enhanced spin-orbit mixing between the ground state and ligand field excited states and thus an increase in *g* anisotropy, as well as a greater localization of the unpaired electron density on the Co(II) ion as reflected in the large A(Co) values.[24, 26, 29]

Interestingly, the small contributions from residual 5C Co(II)Cbl to the EPR spectrum of Co(II)Cbl in the presence of *Lm*EutT and MgATP between 2600 and 3700 G are characteristic of a base-off rather than a base-on Co(II)Cbl species (cf. Figure 5C and 5E). Base-off Co(II)Cbl (which is indistinguishable from Co(II)Cbi$^+$ by EPR spectroscopy) displays a larger g spread than base-on Co(II)Cbl (g_x = 2.48 vs g_x =2.26) and lacks axial superhyperfine coupling due to the substitution of the DMB base by a more weakly electron donating water molecule.[29] Consistent with these EPR data, a closer inspection of the MCD spectrum of Co(II)Cbl in the presence of *Lm*EutT and excess MgATP (Figure S1, Supporting Information) also reveals minor contributions from a small fraction of base-off Co(II)Cbl to the spectral region between 16 000 and 19 000 cm^{-1}. Addition of a larger excess (>10 equiv.) of MgATP did not noticeably change the relative

populations of the 4C and 5C Co(II)Cbl species in the presence of *Lm*EutT and MgATP (Figure 5C and 5D; Table 1), though the exact proportions are difficult to determine due to the large spread of the EPR features associated with 4C Co(II)Cbl.

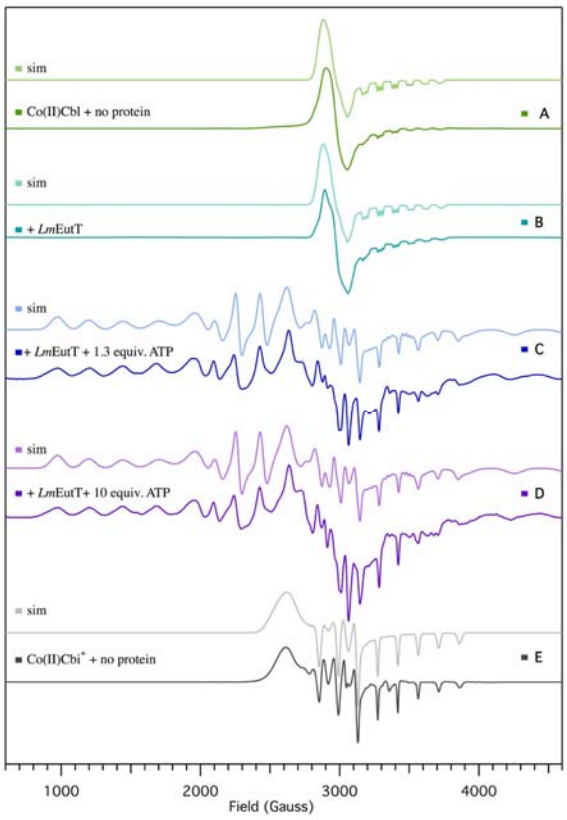

Figure 5. EPR spectra collected at 20 K of **A**) free Co(II)Cbl (green), **B**) Co(II)Cbl incubated with *Lm*EutT (teal), **C**) Co(II)Cbl in the presence of *Lm*EutT and 1.3 equiv. MgATP (blue) or **D**) >10 equiv. MgATP (purple), and **E**) free $Co(II)Cbi^{+}$ (gray). The simulated spectra (labeled "sim" and shown in lighter colors above experimental traces) were obtained using the fit parameters provided in Table 1.

Table 1. Spin-Hamiltonian Parameters for Co(II)Cbl and Co(II)Cbi$^+$ in the Absence and Presence of *Lm*EutT and MgATP

Species	***g* values**			***A* (^{59}Co)/MHz**			***A* (^{14}N)/MHz**
	g_x	g_y	g_z	A_x	A_y	A_z	A_{iso}
A) Co(II)Cbl							
base-on	2.269	2.232	2.004	40	30	302	49
B) Co(II)Cbl + *Lm*EutT							
base-on	2.269	2.233	2.001	40	30	306	49
C) Co(II)Cbl + *Lm*EutT + 1.3/10 equiv. MgATP							
4C species >80%	3.530	2.583	1.800	1265	558	700	n/a
Base-off <20%	2.438	2.300	1.990	210	195	386	
D) Co(II)Cbi$^+$							
Base-off	2.423	2.314	1.994	226	210	402	n/a
E) Co(II)Cbi$^+$ + *Lm*EutT							
Base-off	2.432	2.322	1.990	226	210	405	n/a
F) Co(II)Cbi$^+$ + *Lm*EutT + 10 equiv. MgATP							
Base-off	2.438	2.300	1.990	210	195	386	n/a
G) Co(II)Cbl + *Se*EutT(Zn) + MgATP							
4C species ~58%	3.610	2.553	1.800	1362	625	760	n/a
H) Co(II)Cbl + *Lr*PduO + MgATP							
4C species	2.720	2.700	1.900	595	755	770	n/a
I) Co(II)Cbl + *Se*CobA + MgATP							
4C species	2.730	2.670	2.060	635	590	805	n/a

Parameters for 4C species generated by *Lr*PduO[26], *Se*CobA[23], and *Se*EutT[24] (G–I) are shown for comparison.

The EPR spectra of Co(II)Cbi$^+$ in the absence and presence of *Lm*EutT are almost superimposable, which provides further evidence that this substrate analogue does not bind to the protein in the absence of MgATP (Figure 6A and 6B). Yet, the EPR spectrum of Co(II)Cbi$^+$ incubated with *Lm*EutT in the presence of a large excess of MgATP is slightly different from that of free Co(II)Cbi$^+$, with the most notable difference being the distinctly smaller hyperfine splittings compared to those observed for free Co(II)Cbi$^+$ (Table 1). This result indicates that Co(II)Cbi$^+$ can bind to *Lm*EutT in the presence of MgATP (Figure 6C and Table 1), as inferred from our MCD data. Notably, this enzyme-bound Co(II)Cbi$^+$ species is characterized by *g* and *A* values that are more similar to those of the 5C base-off Co(II)Cbl species contributing to the EPR spectrum of Co(II)Cbl in the presence of *Lm*EutT and MgATP than of free Co(II)Cbi$^+$ (Table 1).

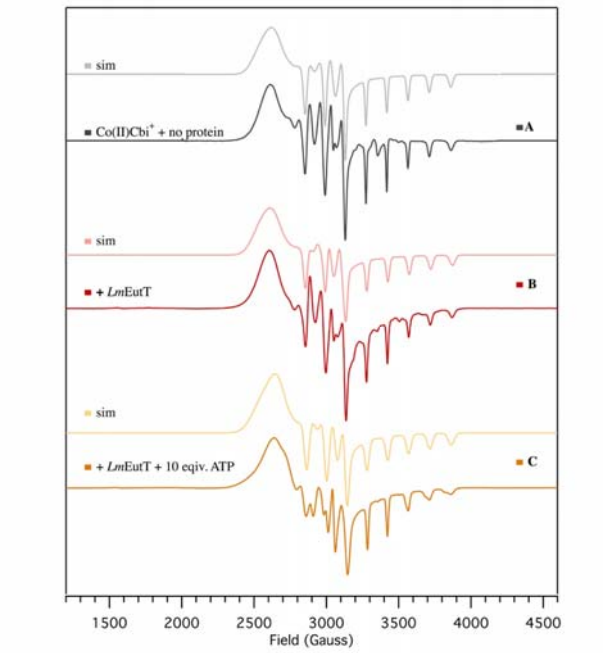

Figure 6. EPR spectra collected at 20 K of **A**) Co(II)Cbi$^+$ (gray), **B**) Co(II)Cbi$^+$ in the presence of *Lm*EutT (red), and **C**) Co(II)Cbi$^+$ in the presence of *Lm*EutT and 10 equiv. MgATP (gold). The simulated spectra (labeled "sim" and shown in lighter colors above experimental traces) were obtained using the fit parameters provided in Table 1.

DISCUSSION

Generation of 4C Co(II)rrinoid Species. ATP:Co(I)rrinoid adenosyltransferases are a group of enzymes involved in the *de novo* synthesis and scavenging of corrinoids to maintain adequate cellular levels of AdoCbl, a biological cofactor used in a variety of enzyme-mediated organic rearrangement and elimination reactions.[11, 12, 45 14, 18] Because a supernucleophilic 4C Co(I)rriniod species is the precursor for the formation of the Co–C bond of AdoCbl, ACATs must be capable of performing the thermodynamically challenging Co(II) → Co(I)Cbl reduction. All ACATs studied to date have been shown to facilitate this reduction by converting the 5C Co(II)Cbl species, normally found in solution, to a unique 4C Co(II)Cbl intermediate in the presence of ATP.[14, 18, 26, 33, 34, 42, 46]

In the present study we have used MCD and EPR spectroscopies to investigate if the EutT-type ACAT from *Listeria monocytogenes* uses the same strategy for Co(II)→ Co(I)rrinoid reduction and to assess the substrate scope of this enzyme. Our data indicate that *Lm*EutT complexed with MgATP can bind Co(II)Cbl as well as Co(II)Cbi$^+$; however, similar to *Se*EutT,[24] this enzyme exclusively converts Co(II)Cbl, and not the Co(II)Cbi$^+$, to a 4C species. Compared to the other ACATs investigated thus far, *Lm*EutT more readily forms a 4C Co(II)Cbl species (>98% 5C→4C conversion yield) on addition of just over one molar equivalent of co-substrate MgATP.[23, 24, 26] In the case of the *Se*EutT, the inability to convert Co(II)Cbi$^+$ to a 4C species was attributed to the presence of a putative binding pocket for the nucleotide loop of Co(II)Cbl to enhance its affinity for the native substrate and promote axial ligand dissociation.[22, 24] The EPR spectrum of Co(II)Cbl in the presence of the *Lm*EutT/MgATP complex reveals that in addition to the major 4C form, a minor 5C, base-off Co(II)Cbl species is generated (Figures 5 and S1). However, this species is unlikely to be catalytically relevant, as its relative population remained constant on

addition of excess MgATP. Thus, unlike *Se*EutT, *Lm*EutT does not appear to generate a 5C, base-off intermediate in the process of 4C Co(II)Cbl formation.[24] This difference in substrate activation mechanism is unsurprising given that *Se*EutT requires a divalent metal cofactor for 4C Co(II)Cbl formation,[22, 24] while *Lm*EutT lacks this cofactor.

Table 2. 5C→ 4C Co(II)rrinoid conversion yields for various ACATs as determined by MCD

Species	% conversion (5C→ 4C)
Co(II)Cbl + *Lm*EutT + 1.3 equiv. ATP	>98
Co(II)Cbl + *Se*EutT (Fe/WT) + >10 equiv. ATP	>85
Co(II)Cbl + *Lr*PduO + ATP	~40
Co(II)Cbi$^+$+ *Lr*PduO + ATP	~50
Co(II)Cbl + *Se*CobA + ATP	~8
Co(II)Cbi$^+$+ *Se*CobA + ATP	~70

Data taken from references as noted: *Lr*PduO[26], *Se*CobA[23], and *Se*EutT[24].

Table 2 summarizes the 5C→ 4C Co(II)rrinoid conversion yields for various ACATs as determined by MCD spectroscopy. The most striking difference among the three ACAT families is that the EutT-type enzymes are unable to convert Co(II)Cbi$^+$ to a 4C species.[23, 24, 26, 29] The crystal structures of 4C Co(II)Cbl bound to *Se*CobA/MgATP and *Lr*PduO/MgATP revealed that these types of ACATs lack specific binding pockets for the nucleotide loop (Figure 2), which allows them to convert both Co(II)Cbl and Co(II)Cbi$^+$ to 4C species.[31, 42] The higher conversion yields with Co(II)Cbi$^+$ (~50% *Lr*PduO, ~70% *Se*CobA) compared to the substrate Co(II)Cbl (~40% *Lr*PduO, 8% *Se*CobA) can be attributed to the more facile removal of the weakly bound water ligand in Co(II)Cbi$^+$ compared to the DMB base in Co(II)Cbl. The high substrate promiscuity displayed by CobA-type ACATs is consistent with the role of these enzymes as part

of the machinery used in the *de novo* biosynthesis of AdoCbl, where scavenging of incomplete corrinoids is likely.[19]

Nature of 4C Co(II)rrinoid Species. All ACATs studied to date raise the Co(II)/Co(I)rrinoid reduction potential to within the physiologically accessible range by generating 4C species, which leads to a stabilization of the "redox-active" Co $3d_{z^2}$ -based MO.[29, 39] Experimental evidence for this orbital stabilization is provided by large shifts of the g_x and g_y values from the free electron value (2.0233) due to enhanced spin-orbit coupling between the ground state and low lying LF (Co $3d_{xz} \rightarrow 3d_{z^2}$ and $3d_{yz} \rightarrow 3d_{z^2}$) excited states.[25, 29] Additionally, the increased localization of the unpaired electron spin density on the Co(II) ion is reflected in the larger $A(^{59}\text{Co})$ hyperfine coupling constants for the 4C Co(II)rrinoid species compared to their 5C counterparts.[24] Interestingly, the 4C Co(II)Cbl species produced in the active sites of *Lm*EutT and *Se*EutT are characterized by much larger $A(^{59}\text{Co})$ hyperfine coupling constants and *g* shifts than those generated by the PduO and CobA type ACATs [$A(^{59}\text{Co})$ EutT ≈ 600–1300 MHz vs $A(^{59}\text{Co})$ PduO/CobA ≈ 600-800 MHz) and g_x (EutT) ≈ 3.6 vs g_x (PduO/CobA) ≈ 2.7].[23, 24, 26] Furthermore, compared to the CobA and PduO-type ACATs, the *g*-tensors of the 4C Co(II)Cbl species generated in the EutT enzymes are much more rhombic ($g_x >> g_y > g_z$), signifying a unique active site environment in the EutT-type ACATs.[24]

In the crystal structures of 4C Co(II)Cbl bound to *Lr*PduO/MgATP and *Se*CobA/MgATP, the corrin ring is relatively planar.[16, 31] Computational studies suggested that for a planar corrin ring conformation, the unpaired electron of 4C Co(II)Cbl resides in the Co $3d_{z^2}$ -based MO that also has large and roughly equal contributions from the Co $3d_{xy}$ and Co $3d_{yz}$ orbitals. This prediction is consistent with the relatively axial *g*-tensors displayed by the 4C Co(II)Cbl species in the *Lr*PduO and *Se*CobA active sites.[29] Thus, the rhombic *g*-tensors exhibited by the EutT-bound

4C Co(II)Cbl species likely reflect a severely constrained conformation of the corrin ring in these enzymes, which would lift the near degeneracy of the Co $3d_{xz}$ and Co $3d_{yz}$-based MOs and result in very different g_x and g_y values. This finding suggests that the corrinoid substrate is firmly locked in place in the EutT active site, which is expected to facilitate the removal of the nucleotide loop during 4C Co(II)Cbl formation.

The results obtained in this study indicate that *Lm*EutT employs a different mechanism than *Se*EutT for controlling the timing of Co(II)Cbl binding and its subsequent conversion to a 4C species. While *Se*EutT can bind Co(II)Cbl in the absence of ATP and convert it to a 5c base-off species with an axial water ligand (Figure 7A), *Lm*EutT must first bind ATP and then Co(II)Cbl, which is directly converted to a 4C species (Figure 7B). Given the identical substrate specificities of *Lm*EutT and *Se*EutT, it is reasonable to suggest that both enzymes possess similar nucleotide binding pockets, though in the case of *Se*EutT the architecture of this putative binding pocket appears to change in response to Fe(II) or Zn(II) ion binding.[24] While the exact role of the divalent metal cofactor of *Se*EutT remains unclear, the fact that the Fe(II)-bound enzyme is deactivated in the presence of molecular oxygen suggests that it may serve as a redox sensor to control the levels of AdoCbl generated under aerobic and anaerobic conditions. The absence of this metal cofactor in *Lm*EutT exemplifies an interesting phylogenetic divergence amongst the EutT enzymes investigated so far.

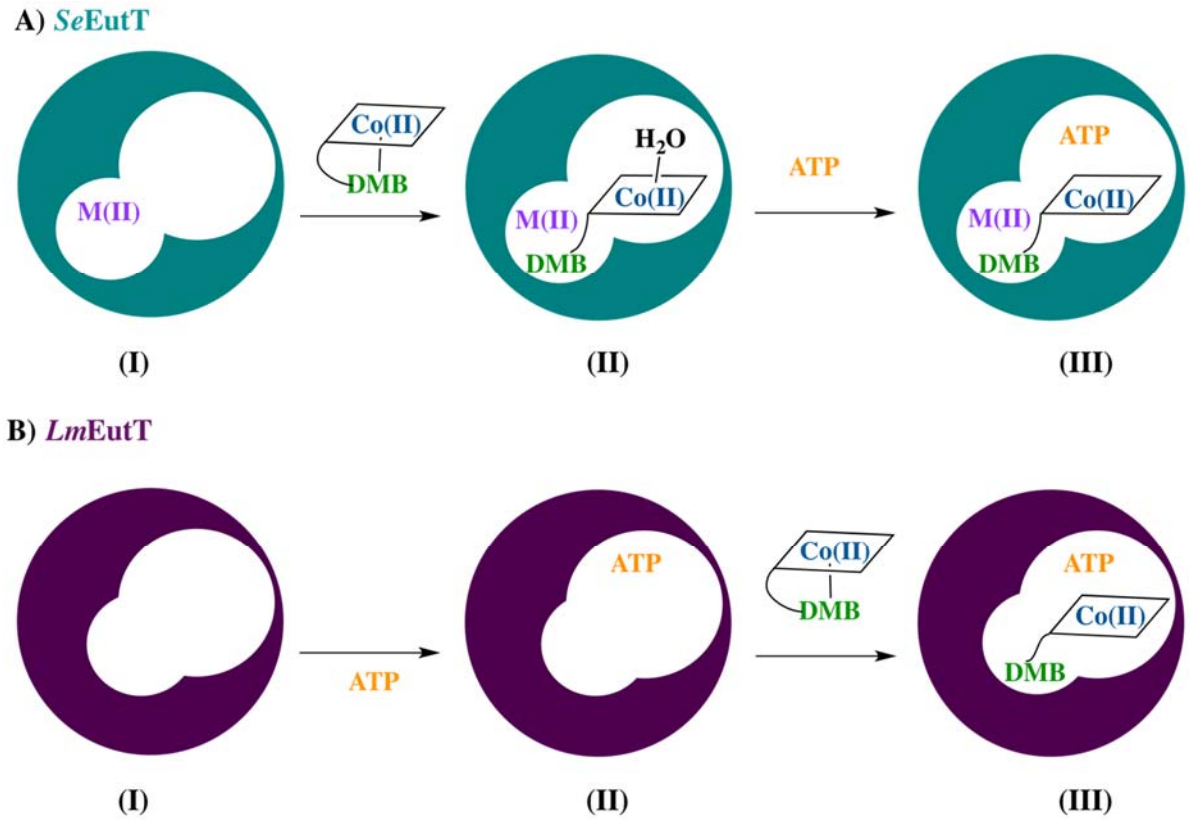

Figure 7. Proposed mechanisms for generation of 4C Co(II)Cbl in the EutT ACATs. In the case of *Se*EutT (A) Co(II)Cbl can bind to the active site in the absence of ATP as long as the divalent metal cofactor is present (I) to yield a base-off species with an axial water ligand (II). This process is facilitated by the binding of the DMB tail to a specific protein pocket. The subsequent binding of ATP then triggers the formation of 4C Co(II)Cbl (III). For *Lm*EutT (**B**) that lacks a divalent metal cofactor (I), the enzyme must first bind ATP (II) and then Co(II)Cbl, which is directly converted to a 4C species whereby the DMB base is sequestered in a binding pocket (III).

SUPPORTING INFORMATION

Near-IR region of the MCD spectra of Co(II)Cbl and Co(II)Cbi$^+$ in the presence of *Lm*EutT and co-substrate MgATP. This material is available free of charge via the Internet at http://pubs.acs.org.

CONFLICT OF INTEREST

The authors declare no competing financial interest

AUTHOR INFORMATION

Corresponding author: brunold@chem.wisc.edu

REFERENCES

1. Garsin, D. A., Ethanolamine utilization in bacterial pathogens: roles and regulation. *Nature Reviews Microbiology* **2010,** *8* (4), 290-295.
2. Chang, G. W.; Chang, J. T., Evidence for the B12-dependent enzyme ethanolamine deaminase in Salmonella. *Nature* **1975,** *254* (5496), 150-151.
3. Del Papa, M. F.; Perego, M., Ethanolamine activates a sensor histidine kinase regulating its utilization in Enterococcus faecalis. *Journal of Bacteriology* **2008,** *190* (21), 7147-7156.
4. Blackwell, C. M.; Scarlett, F. A.; Turner, J. M., Ethanolamine catabolism by bacteria, including Escherichia coli. Portland Press Limited: 1976.
5. Randle, C. L.; Albro, P. W.; Dittmer, J. C., The phosphoglyceride composition of Gram-negative bacteria and the changes in composition during growth. *Biochimica et Biophysica Acta (BBA)-Lipids and Lipid Metabolism* **1969,** *187* (2), 214-220.
6. Ansell, G. B.; Hawthorne, J. N.; Dawson, R. M. C. Elsevier Scientific Pub. Co,: New York, Amsterdam, **1973**, page 289.
7. Larson, T. J.; Ehrmann, M.; Boos, W., Periplasmic glycerophosphodiester phosphodiesterase of Escherichia coli, a new enzyme of the glp regulon. *Journal of Biological Chemistry* **1983,** *258* (9), 5428-5432.

8. Proulx, P.; Fung, C. K., Metabolism of phosphoglycerides in *E. coli* IV. The positional specificity and properties of phospbolipase A. *Canadian journal of biochemistry* **1969,** *47* (12), 1125-1128.

9. Bradbeer, C., The clostridial fermentations of choline and ethanolamine I. Preparation and properties of cell-free extracts. *Journal of Biological Chemistry* **1965,** *240* (12), 4669-4674.

10. Jones, P. W.; Turner, J. M., Interrelationships between the enzymes of ethanolamine metabolism in *Escherichia coli*. *Microbiology* **1984,** *130* (2), 299-308.

11. Banerjee, R., Ed., Chemistry and Biochemistry of B_{12}. John Wiley & Sons, INC: New York, NY, 1999.

12. Banerjee, R., Radical Peregrinations Catalyzed by Coenzyme B_{12}-Dependent Enzymes. *Biochemistry* **2001,** *40* (29), 8634-8634.

13. Banerjee, R.; Ragsdale, S. W., The Many Faces of Vitamin B_{12}: Catalysis by Cobalamin-Dependent Enzymes. *Annual Review of Biochemistry* **2003,** *72*, 209-247.

14. Mera, P. E.; Escalante-Semerena, J. C., Multiple roles of ATP:cob(I)alamin adenosyltransferases in the conversion of B_{12} to coenzyme B_{12}. *Applied microbiology and biotechnology* **2010,** *88* (1), 41-48.

15. Mera, P. E.; St Maurice, M.; Rayment, I.; Escalante-Semerena, J. C., Structural and Functional Analyses of the Human-Type Corrinoid Adenosyltransferase (PduO) from *Lactobacillus reuteri*. *Biochemistry* **2007,** *46* (48), 13829-13836.

16. Mera, P. E.; St Maurice, M.; Rayment, I.; Escalante-Semerena, J. C., Residue Phe112 of the Human-Type Corrinoid Adenosyltransferase (PduO) Enzyme of *Lactobacillus reuteri* Is Critical to the Formation of the Four-Coordinate Co(II) Corrinoid Substrate and to the Activity of the Enzyme. *Biochemistry* **2009,** *48* (14), 3138-3145.

17. Johnson, C. L. V.; Pechonick, E.; Park, S. D.; Havemann, G. D.; Leal, N. A.; Bobik, T. A., Functional genomic, biochemical, and genetic characterization of the Salmonella pduO gene, an ATP: cob (I) alamin adenosyltransferase gene. *Journal of bacteriology* **2001,** *183* (5), 1577-1584.

18. Warren, M. J.; Raux, E.; Schubert, H. L.; Escalante-Semerena, J. C., The biosynthesis of adenosylcobalamin (vitamin B12). *Natural product reports* **2002,** *19* (4), 390-412.

19. Escalante-Semerena, J. C.; Suh, S. J.; Roth, J. R., cobA Function is required for both de novo cobalamin biosynthesis and assimilation of exogenous corrinoids in Salmonella typhimurium. *Journal of Bacteriology* **1990,** *172*, 273-280.

20. Moore, T. C.; Mera, P. E.; Escalante-Semerena, J. C., The EutT Enzyme of *Salmonella enterica* is a Unique ATP:Cob(I)alamin Adenosyltransferase Metalloprotein that Requires Ferrous Ions for Maximal Activity. *Journal of bacteriology* **2014,** *196* (4), 903-910.

21. Buan, N. R.; Suh, S.-J.; Escalante-Semerena, J. C., The *eutT* Gene of *Salmonella enterica* Encodes an Oxygen-Labile, Metal-Containing ATP:Corrinoid Adenosyltransferase Enzyme. *Journal of bacteriology* **2004,** *186* (17), 5708-5714.

22. Pallares, I. G.; Moore, T. C.; Escalante-Semerena, J. C.; Brunold, T. C., Spectroscopic Studies of the EutT Adenosyltransferase from *Salmonella enterica*: Evidence for a Tetrahedrally Coordinated Divalent Transition Metal Cofactor with Cysteine Ligation. *Biochemistry* **2017,** *56* (2), 364-375.

23. Pallares, I. G.; Moore, T. C.; Escalante-Semerena, J. C.; Brunold, T. C., Spectroscopic Studies of the *Salmonella enterica* Adenosyltransferase Enzyme *Se*CobA: Molecular-Level Insight into the Mechanism of Substrate Cob(II)alamin Activation. *Biochemistry* **2014,** *53* (50), 7969-7982.

24. Pallares, I. G.; Moore, T. C.; Escalante-Semerena, J. C.; Brunold, T. C., Spectroscopic Studies of the EutT Adenosyltransferase from *Salmonella enterica*: Mechanism of Four-Coordinate Co(II)Cbl Formation. *Journal of the American Chemical Society* **2016,** *138* (1), 3694-3704.

25. Brunold, T. C.; Conrad, K. S.; Liptak, M. D.; Park, K., Spectroscopically validated density functional theory studies of the B12 cofactors and their interactions with enzyme active sites. *Coordination Chemistry Reviews* **2009,** *253* (5), 779-794.

26. Park, K.; Mera, P. E.; Escalante-Semerena, J. C.; Brunold, T. C., Kinetic and Spectroscopic Studies of the ATP:Corrinoid Adenosyltransferase PduO from *Lactobacillus reuteri*: Substrate Specificity and Insights into the Mechanism of Co(II)corrinoid Reduction. *Biochemistry* **2008,** *47* (34), 9007-9015.

27. Park, K.; Mera, P. E.; Moore, T. C.; Escalante-Semerena, J. C.; Brunold, T. C., Unprecedented Mechanism Employed by the *Salmonella enterica* EutT ATP:Co^{I}rrinoid Adenosyltransferase Precludes Adenosylation of Incomplete Co^{II}rrinoids. *Angewandte Chemie International Edition* **2015,** *54* (24), 7158-7161.

28. Liptak, M. D.; Fleischhacker, A. S.; Matthews, R. G.; Telser, J.; Brunold, T. C., Spectroscopic and Computational Characterization of the Base-off Forms of Cob (II) alamin. *The Journal of Physical Chemistry. B* **2009,** *113* (15), 5245-5254.

29. Stich, T. A.; Buan, N. R.; Escalante-Semerena, J. C.; Brunold, T. C., Spectroscopic and Computational Studies of the ATP:Corrinoid Adenosyltransferase (CobA) from *Salmonella enterica*: Insights into the Mechanism of Adenosylcobalamin Biosynthesis. *Journal of the American Chemical Society* **2005,** *127* (24), 8710-8719.

30. Stich, T. A.; Yamanishi, M.; Banerjee, R.; Brunold, T. C., Spectroscopic Evidence for the Formation of a Four-Coordinate Co^{2+} Cobalamin Species upon Binding to the Human ATP:Cobalamin Adenosyltransferase. *Journal of the American Chemical Society* **2005,** *127* (21), 7660-7661.

31. Moore, T. C.; Newmister, S. A.; Rayment, I.; Escalante-Semerena, J. C., Structural Insights into the Mechanism of Four-Coordinate Cob(II)alamin Formation in the Active Site of the Salmonella enterica ATP:Co(I)rrinoid Adenosyltransferase Enzyme: Critical Role of Residues Phe91 and Trp93. *Biochemistry* **2012,** *51* (48), 9647-9657.

32. Faure, D.; Lexa, D.; Savéant, J.-M., Electrochemistry of vitamin B_{12}: Part IX. The Co (III)/Co (II) couple in non-aqueous solvents. *Journal of Electroanalytical Chemistry and Interfacial Electrochemistry* **1982,** *140* (2), 297-309.

33. Mera, P. E.; Escalante-Semerena, J. C., Dihydroflavin-driven Adenosylation of 4-Coordinate Co(II)corrinoids are cobalamin reductases: Enzymes or electron transfer proteins? *Journal of Biological Chemistry* **2010,** *285* (5), 2911-2917.

34. Liptak, M. D.; Brunold, T. C., Spectroscopic and Computational Studies of Co^{1+}Cobalamin: Spectral and Electronic Properties of the "Superreduced" B_{12} Cofactor. *Journal of the American Chemical Society* **2006,** *128* (28), 9144-9156.

35. Costa, F. G.; Escalante-Semerena, J. C., A new class of EutT ATP:Co(I)rrinoid adenosyltransferases found in *Listeria monocytogenes* and other *Firmicutes* does not require a metal ion for activity. *Biochemistry* **2018,** *Submitted*.

36. Maniatis, T.; Fritsch, E. F.; Sambrook, J., *Molecular cloning: a laboratory manual*. Cold Spring harbor laboratory Cold Spring Harbor, NY: 1982; Vol. 545.

37. Blommel, P. G.; Becker, K. J.; Duvnjak, P.; Fox, B. G., Enhanced bacterial protein expression during auto-induction obtained by alteration of lac repressor dosage and medium composition. *Biotechnology progress* **2007,** *23* (3), 585-598.

38. Nilges, M. J. Thesis in Chemistry. University of Illinois, Urbana-Champaign, Il, 1979.

39. Stich, T. A.; Buan, N. R.; Brunold, T. C., Spectroscopic and computational studies of Co^{2+}corrinoids: Spectral and electronic properties of the biologically relevant base-on and base-off forms of Co^{2+}cobalamin. *Journal of the American Chemical Society* **2004,** *126* (31), 9735-9749.

40. Pratt, J. M., *Inorganic Chemistry of Vitamin B12*. Academic Press Inc.(London) Ltd.: London, UK, 1972.

41. Brooks, A. J.; Vlasie, M.; Banerjee, R.; Brunold, T. C., Co-C Bond Activation in Methylmalonyl-CoA Mutase by Stabilization of the Post-Homolysis Product Co^{2+}Cobalamin. *Journal of the American Chemical Society* **2005,** *127* (47), 16522-16528.

42. Park, K.; Mera, P. E.; Escalante-Semerena, J. C.; Brunold, T. C., Spectroscopic Characterization of Active-site Variants of the PduO-type ATP:Corrinoid Adenosyltransferase from *Lactobacillus reuteri*: Insights into the Mechanism of Four-Coordinate Co(II)corrinoid Formation. *Inorganic chemistry* **2012,** *51* (8), 4482-4494.

43. Andruniow, T.; Zgierski, M. Z.; Kozlowski, P. M., Vibrational analysis of methylcobalamin. *The Journal of Physical Chemistry A* **2002,** *106* (7), 1365-1373.

44. Palmer, G., In *Physical Methods in Bioinorganic Chemistry*, Sausalito, CA, 2000; p 121.

45. Banerjee, R., Radical Carbon Skeleton Rearrangements: Catalysis by Coenzyme B_{12}-Dependent Mutases. *Chemical Reviews* **2003,** *103* (6), 2083-2094.

46. Fonseca, M. V.; Escalante-Semerena, J. C., Reduction of Cob(III)alamin to Cob(II)alamin in *Salmonella enterica* Serovar Typhimurium LT2. *Journal of Bacteriology* **2000,** *182* (15), 4304-4309.

For Table of Contents Use Only

Spectroscopic Study of the EutT Adenosyltransferase from *Listeria monocytogenes*: Evidence for the Formation of a Four-Coordinate Cob(II)alamin Intermediate.

Nuru G. Stracey, Flavia G. Costa, Jorge C. Escalante-Semerena, and Thomas C. Brunold